

Determination of Antiferromagnetic Exchange Coupling in the Tetrahedral Thiolate-Bridged Diferrous Complex $[\text{Fe}_2(\text{SEt})_6]^{2-}$

Yiannis Sanakis,^{†,‡} Sun Jae Yoo,[†] Frank Osterloh,^{§,||} R. H. Holm,[§] and Eckard Münck^{*,†}

Department of Chemistry, Carnegie Mellon University, Pittsburgh, Pennsylvania 15213, Institute of Materials Science, NCSR “Demokritos”, 15310 Ag. Paraskevi, Attiki, and Department of Biological Applications and Technologies, University of Ioannina, 45110 Ioannina, Greece, Department of Chemistry and Chemical Biology, Harvard University, Cambridge, Massachusetts 02138, and Department of Chemistry, University of California, Davis, California 95616

Received July 16, 2002

Protein-bound iron–sulfur clusters and their synthetic analogues are characterized by tetrahedral metal sites, multiple oxidation levels, and exchange coupling. The recent attainment of several all-ferrous protein clusters and the presence of sulfide- and thiolate-bridged sites in the all-ferrous state of the nitrogenase P-cluster provides an imperative for determination of exchange coupling between tetrahedral Fe(II) sites with sulfur bridges. The cluster in the previously reported compound $(\text{Et}_4\text{N})_2[\text{Fe}_2(\text{SEt})_6]$ is centrosymmetric with distorted tetrahedral coordination and a planar Fe_2 - $(\mu\text{-SEt})_2$ bridge unit. The compound is diamagnetic at 4.2 K, indicating antiferromagnetic coupling. The lower limit $J > 80 \text{ cm}^{-1}$ ($H = JS_1 \cdot S_2$) is obtained by Mössbauer spectroscopy. Analysis of magnetic susceptibility data affords $J = 165 \pm 15 \text{ cm}^{-1}$. It is noteworthy that the J value of the diferrous pair obtained here is comparable to the J values reported for the mixed-valence state of plant-type Fe_2S_2 ferredoxins. The near temperature independence of the quadrupole splitting ($\Delta E_Q = 3.25 \text{ mm/s}$ at 4.2 K and 3.20 mm/s at 180 K) indicates that no excited orbital states are appreciably populated at temperatures less than 300 K. The paramagnetism arises solely from thermal population of the $S = 1$ state of the spin ladder. This work provides the only measure of antiferromagnetic coupling by Fe(II) pairs in a tetrahedral sulfur environment.

Introduction

The established cluster core structures in iron–sulfur proteins¹ are rhombic Fe_2S_2 , cuboidal Fe_3S_4 , cubane-type Fe_4S_4 , and the bridged double-cubane Fe_8S_7 (P-cluster) of nitrogenase.^{2–4} These clusters contain distorted tetrahedral FeS_4 sites and exhibit multiple oxidation states. The geo-

metric and electronic structures of the more oxidized states have been extensively studied and are now rather thoroughly elucidated. Recently, reduced states have been attained and electronically characterized in several proteins. The diferrous $[\text{Fe}_2\text{S}_2]^0$ state of a ferredoxin isolated from *Aquifex aeolicus* was demonstrated by Mössbauer spectroscopy.⁵ The all-ferrous $[\text{Fe}_4\text{S}_4]^0$ state has been attained in the Fe protein of the *Azotobacter vinelandii* nitrogenase system.^{6,7} These states are to be distinguished from $[\text{Fe}_2\text{S}_2]^{2+/+}$ and $[\text{Fe}_4\text{S}_4]^{3+/2+/+}$, which are all- Fe^{3+} or mixed-valence $\text{Fe}^{3+}/\text{Fe}^{2+}$ oxidation levels implicated in the usual physiological redox couples of iron–sulfur proteins.

Iron–sulfur clusters in all oxidation levels are exchange-coupled systems with spectroscopic properties that reflect

* Author to whom correspondence should be addressed. E-mail: emunck@cmu.edu. Fax: (412) 268 1061.

[†] Carnegie Mellon University.

[‡] Institute of Materials Science, NCSR “Demokritos”, and Department of Biological Applications and Technologies, University of Ioannina.

[§] Harvard University.

^{||} University of California.

- (1) Beinert, H.; Holm, R. H.; Münck, E. *Science* **1997**, *277*, 653.
- (2) Bolin, J. T.; Campobasso, N.; Muchmore, S. W.; Morgan, T. V.; Mortenson, L. E. In *Molybdenum Enzymes, Cofactors, and Model Systems*; Stiefel, E. I., Coucouvanis, D., Newton, W. E., Eds.; American Chemical Society: Washington, DC, 1993; p 186.
- (3) Peters, J. W.; Stowell, M. H. B.; Soltis, S. M.; Finnegan, M. G.; Johnson, M. K.; Rees, D. C. *Biochemistry* **1997**, *36*, 1181.
- (4) Mayer, S. M.; Lawson, D. M.; Gormal, C. A.; Roe, S. M.; Smith, B. E. *J. Mol. Biol.* **1999**, *292*, 871.

(5) Yoo, S. J.; Meyer, J.; Münck, E. *J. Am. Chem. Soc.* **1999**, *121*, 10450.

(6) Angove, H. C.; Yoo, S. J.; Burgess, B. K.; Münck, E. *J. Am. Chem. Soc.* **1997**, *119*, 8730.

(7) Yoo, S. J.; Angove, H. C.; Burgess, B. K.; Hendrich, M. P.; Münck, E. *J. Am. Chem. Soc.* **1999**, *121*, 2534.

the oxidation states of the metals as well as details of the specific coupling. The exchange interactions involve Fe^{3+} - Fe^{3+} , $\text{Fe}^{2+}\text{Fe}^{3+}$, or $\text{Fe}^{2+}\text{Fe}^{2+}$ pairs. For the mixed-valence pairs, both Heisenberg–Dirac–van Vleck ($H = JS_1 \cdot S_2$) and double exchange have to be considered. For a polynuclear cluster, it is very difficult to extract a reliable set of J values from magnetization studies. As one example, the determination of the exchange couplings of $[\text{Fe}_4\text{S}_4]^{2+}$ clusters requires specification of six J values and at least two double exchange coupling constants. We have, therefore, searched for systems containing only *one* exchange-coupled Fe–Fe pair in environments that resemble those encountered in certain protein-bound clusters. We have obtained the value $J(\text{Fe}^{3+}\text{Fe}^{3+}) = 280 \text{ cm}^{-1}$ by studying the cubane-type cluster $[\text{Fe}_4\text{S}_4(\text{SEt})_2(\text{BuNC})_6]$, in which two Fe(II) sites are rendered diamagnetic by isonitrile coordination.⁸ For the antiferromagnetically coupled $[\text{Fe}_2\text{S}_2]^0$ state of *A. aeolicus* ferredoxin, we determined from Mössbauer spectroscopy the lower limit $J(\text{Fe}^{2+}\text{Fe}^{2+}) = +80 \text{ cm}^{-1}$.⁵

The P-cluster of nitrogenase can be considered as a double cubane linked by two bridging cysteinates and a common sulfide.^{3,4} In the reduced, all-ferrous state P^{N} the bridging sulfide is μ_6 while in the two-electron-oxidized form P^{OX} it is μ_4 . In the P^{N} state, the Fe–Fe distances in the two bridged $\text{Fe}_2(\mu_6\text{-S})(\mu_2\text{-S}\cdot\text{Cys})$ fragments are 2.92–3.05 Å in the proteins from *A. vinelandii* and *Klebsiella pneumoniae*. In the P^{OX} state, one distance decreases slightly to 2.97–2.99 Å while the other increases to 3.74–3.79 Å in the formation of the $\text{Fe}_2(\mu_4\text{-S})(\mu_2\text{-S}\cdot\text{Cys})$ fragment.^{3,4} Mousesca et al.⁹ have analyzed spin coupling in the state P^{OX} . This state comprises six Fe^{2+} and two Fe^{3+} sites, and in the coupling scheme of Mousesca et al. all six bridging irons are ferrous. In analyzing published magnetic hyperfine interactions reported from Mössbauer studies of P^{OX} , Mousesca et al. assumed that the coupling between the cubanes is weak compared to the coupling within each cubane. It is known that the exchange coupling of two Fe^{3+} ions linked by a single sulfido bridge can be considerable: $J \approx 180 \text{ cm}^{-1}$ in $[\text{Fe}(\text{salen})]_2\text{S}$.¹⁰ The oxidation state of the iron components of the M (cofactor) cluster MoFe_7S_9 of nitrogenase is still uncertain. For the M^{N} ($S = 3/2$) state, either $6\text{Fe}^{2+}\text{Fe}^{3+}$ ¹¹ or $4\text{Fe}^{2+}3\text{Fe}^{3+}$ ¹² is compatible with present data.¹³

In the absence of suitable model complexes, the inter-cubane coupling of the P-cluster is difficult to assess. To proceed further with this and related problems involving reduced clusters, information on the strength of coupling between pairs of tetrahedral Fe^{2+} sites bridged by sulfide and/or thiolate would be useful. Pertinent data, however, have

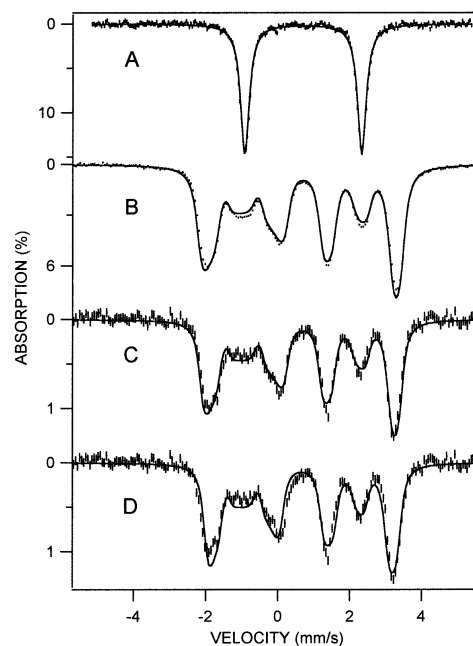


Figure 1. Mössbauer spectra of polycrystalline $(\text{Et}_4\text{N})_2[\text{Fe}_2(\text{SEt})_6]$ recorded at 4.2 K (A, B) and 180 K (C, D) in zero field (A) and in an 8.0 T field (B, C, D) applied parallel to the observed γ -radiation. The solid lines are spectral simulations based on eq 1 using, for both sites, $D = 5.7 \text{ cm}^{-1}$, $E/D = 0.25$, $g_x = g_y = 2.08$, $g_z = 2.00$, $A_x = -20.1 \text{ MHz}$, $A_y = -11.3 \text{ MHz}$, $A_z = -33.4 \text{ MHz}$, $\delta = 0.70 \text{ mm/s}$, $\Delta E_Q = -3.25 \text{ mm/s}$ at 4.2 K and $\Delta E_Q = -3.20 \text{ mm/s}$ at 180 K, and $\eta = 0.65$. For spectra B and C we employed $J = 165 \text{ cm}^{-1}$, and for spectrum D we employed $J = 50 \text{ cm}^{-1}$. The same electronic parameters were used for generating the theoretical curves in Figure 2.

not been reported. As part of a systematic study of Fe(II) thiolate complexes, the compound $(\text{Et}_4\text{N})_2[\text{Fe}_2(\text{SEt})_6]$ was prepared and structurally characterized.¹⁴ Because of crystallographically imposed centrosymmetry, the complex has the advantage of equivalent iron sites, with distorted tetrahedral coordination, a planar $\text{Fe}_2(\mu\text{-S})_2$ bridge unit with ethyl groups in the anti conformation, and an iron–iron separation of 2.978(1) Å. We report here the Mössbauer spectroscopic and magnetic properties of this complex.

Experimental Section

The compound $(\text{Et}_4\text{N})_2[\text{Fe}_2(\text{SEt})_6]$, **1**, was prepared by a published method.¹⁴ All measurements were carried out under strictly anaerobic conditions. Mössbauer spectra were recorded with a constant acceleration spectrometer equipped with a Janis Research cryostat and a superconducting magnet that allows application of magnetic fields up to 8.0 T parallel to the incident γ -rays. Isomer shifts are referenced to iron metal at 298 K. Magnetic measurements were made with a MPMS Quantum Design SQUID susceptometer calibrated with a palladium standard. The Mössbauer spectra were analyzed with the software package WMOSS (WEB Research Co., Edina, MN). The data of Figure 2 were analyzed with a program that generates the powder susceptibility based on the electronic terms of eq 1.

Results

(a) Mössbauer Spectra. Shown in Figure 1A is a Mössbauer spectrum of polycrystalline $(\text{Et}_4\text{N})_2[\text{Fe}_2(\text{SEt})_6]$,

(8) Yoo, S. J.; Hu, Z.; Goh, C.; Bominaar, E. L.; Holm, R. H.; Münck, E. *J. Am. Chem. Soc.* **1997**, *119*, 8732.

(9) Mousesca, J.-M.; Noodleman, L.; Case, D. A. *Inorg. Chem.* **1994**, *33*, 4819.

(10) Dorfman, J. R.; Girerd, J.-J.; Simhom, E. D.; Stack, T. D. P.; Holm, R. H. *Inorg. Chem.* **1984**, *23*, 4407.

(11) Lee, H.-I.; Hales, B. J.; Hoffman, B. M. *J. Am. Chem. Soc.* **1997**, *119*, 11395.

(12) Yoo, S.-J.; Angove, H. C.; Burgess, B. K.; Münck, E. *J. Am. Chem. Soc.* **2000**, *122*, 4926.

(13) Lovell, T.; Li, J.; Case, D. E.; Noodleman, L. *J. Am. Chem. Soc.* **2001**, *123*, 12392.

(14) Hagen, K. S.; Holm, R. H. *Inorg. Chem.* **1984**, *23*, 418.

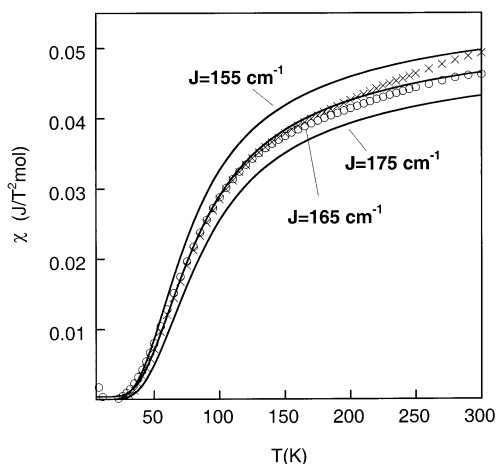


Figure 2. Plot of the temperature dependence of the magnetic susceptibility of polycrystalline $(\text{Et}_4\text{N})_2[\text{Fe}_2(\text{SEt})_6]$. Data were recorded at 3.0 T (O) and 5.0 T (X) applied fields. Two minor contaminants, each perhaps representing 0.4% of total iron, and the diamagnetism of the sample holder were fitted to the equation $\chi = A/T + B$, with $A = 0.26 \text{ J K/T mol}$ and $B = 0.033 \text{ J/T}^2 \text{ mol}$ (at 3.0 T), and their contributions were subtracted from the raw data. The solid line drawn through the data is a fit based on eq 1 for $J = 165 \text{ cm}^{-1}$. For comparison, simulated curves for $J = 155 \text{ cm}^{-1}$ and $J = 175 \text{ cm}^{-1}$ are also shown. The small differences between the 3.0 and 5.0 T data for $T > 150 \text{ K}$ may indicate that the assumptions about the assumed impurities are not strictly correct.

1, recorded at 4.2 K in the absence of an applied magnetic field. The spectrum consists of a symmetric doublet with quadrupole splitting $\Delta E_Q = 3.25 \pm 0.02 \text{ mm/s}$ and isomer shift $\delta = 0.70 \pm 0.02 \text{ mm/s}$. These values are typical for high-spin Fe^{2+} in a distorted tetrahedral environment of thiolate ligands.¹⁵ The quadrupole splitting is essentially independent of temperature; thus, at 180 K we observed $\Delta E_Q = 3.20 \text{ mm/s}$. The spectrum shown in Figure 1B was recorded at 4.2 K in a field of 8.0 T applied parallel to the γ -rays. The solid line is a spectral simulation based on the assumption that both irons of **1** reside in a diamagnetic environment. The good fit of the theoretical curve to the experimental data supports this assumption. Because the two irons are intrinsically high-spin Fe^{2+} , the observation of a diamagnetic ground state shows that the two iron sites are antiferromagnetically coupled. The simulations also suggest that both iron sites are equivalent, in accord with the crystallographic information; for both sites we obtained $\Delta E_Q < 0$ and asymmetry parameter $\eta = 0.65$.

In order to estimate the exchange coupling constant J with Mössbauer spectroscopy, we have recorded 8.0 T spectra at temperatures up to 180 K. The 180 K spectrum is shown in Figure 1C and Figure 1D. At sufficiently high temperatures, excited states with $S > 0$ (essentially the $S = 1$ level) of the spin ladder become populated. These paramagnetic states will contribute magnetic hyperfine structure when the samples are studied in applied magnetic fields. If the electron spin relaxes slowly, population of states with $S > 0$ would manifest itself by the appearance of additional spectral components. For fast spin relaxation, however, only one

spectrum would be observed. The latter situation applies to the 180 K spectrum of Figure 1C.

Kauffmann and Münck¹⁶ have shown how the exchange coupling constant, J , of a dimer can be determined by variable-temperature, high-field Mössbauer spectroscopy (this method works very well for $J < 80 \text{ cm}^{-1}$). For the present case we can describe the Mössbauer spectra with the spin Hamiltonian ($S_1 = S_2 = 2$),

$$H = JS_1 \cdot S_2 + \sum_{j=1,2} \{ \mathbf{S}_j \cdot \mathbf{D}_j \cdot \mathbf{S}_j + \beta \mathbf{S}_j \cdot \mathbf{g}_j \cdot \mathbf{B} + \mathbf{S}_j \cdot \mathbf{A}_j \cdot \mathbf{I}_j - g_n \beta_n \mathbf{B} \cdot \mathbf{I}_j + H_Q(j) \} \quad (1)$$

where j sums over the two (equivalent) iron sites. \mathbf{D}_j is the zero-field splitting tensor of site j (principal values D_j and E_j), \mathbf{g}_j is the electronic \mathbf{g} -tensor, \mathbf{A}_j is the magnetic hyperfine tensor, and $H_Q(j)$ describes the interaction of the electric field gradient (EFG) tensor with the nuclear quadrupole moment; V_{xx} , V_{yy} , and V_{zz} are the principal components of the EFG tensor, and $\eta = (V_{xx} - V_{yy})/V_{zz}$ is the asymmetry parameter (we have dropped the site index j). Because of the inversion symmetry of **1**, the local tensors of the two sites have to be the same. At temperatures for which states of the spin ladder with $S > 0$ are populated, the magnetic splittings of the Mössbauer spectra depend on the \mathbf{A} -tensors and (although less sensitively) on the g and D values. The 4.2 K spectrum of Figure 1B is independent of the A values (only the $S = 0$ state is populated).

We have recently completed a comprehensive analysis of the Mössbauer spectra of the tetrathiolate site of ferrous rubredoxin, Rd_{red} .¹⁷ Not surprisingly, the values of ΔE_Q , δ , and η obtained here are virtually the same as those of Rd_{red} . Thus, it is reasonable to assume that the A values of **1** are also similar to those of Rd_{red} . Moreover, we will assume that **1** and Rd_{red} have the same zero-field splitting parameters, namely, $D_j = 5.7 \text{ cm}^{-1}$ and $(E/D)_j = 0.25$.¹⁷ The solid line drawn through the data of Figure 1D is a simulation generated from eq 1 for $J = 50 \text{ cm}^{-1}$. It can be seen that the splitting of the low-energy feature of the theoretical spectrum is smaller than that of the experimental one. This indicates that the population of the $S = 1$ level, which produces an internal magnetic field opposed to the applied field, is less than assumed in the calculation, and thus J must be larger than 50 cm^{-1} . By performing simulations with larger J values we have established by Mössbauer spectroscopy a lower limit $J > 80 \text{ cm}^{-1}$. The simulation shown in Figure 1C will be discussed below.

(b) Magnetization Data. Shown in Figure 2 is the temperature dependence of magnetic susceptibility of polycrystalline **1** obtained in applied fields of 3.0 T (O) and 5.0 T (X). The sample studied was from the same batch as that used for the Mössbauer measurements. Our analysis revealed

(15) Münck, E. In *Physical Methods in Inorganic and Bioinorganic Chemistry*; Que, L., Jr., Ed.; University Science Books: Sausalito, CA, 2000; Chapter 6.

(16) Kauffmann, K. E.; Münck, E. In *Spectroscopic Methods in Bioinorganic Chemistry*; Solomon, E. I., Hodgson, K., Eds.; ACS Symposium Series 692; American Chemical Society: Washington, DC, 1998; p 16.

(17) Vrajmasu, V. V.; Bominaar, E. L.; Meyer, J.; Münck, E. *Inorg. Chem.*, in press.

the presence of two minor contaminants. First, the sample contained a paramagnetic impurity. Its contribution was recognizable by the rising susceptibility behavior below ca. 40 K; if this contaminant were mononuclear high-spin Fe(II) ($S = 2$), it would represent 0.4% of the iron in the sample. Second, the sample appeared to contain a minor ferromagnetic contaminant having an apparent Curie temperature above 300 K. Such a contaminant would produce a temperature-independent susceptibility behavior that scales with the applied field; this was indeed observed. If we assume arbitrarily that this ferromagnetic contaminant contains only high-spin Fe(II), it would represent ca. 0.4% of the total iron in the sample. At these concentrations the two contaminants would be difficult to detect by Mössbauer spectroscopy. Finally, the measured susceptibility contains a diamagnetic contribution from the sample holder that was determined by blank runs at 3.0 and 5.0 T. We have fitted the contributions of the gel cap and of the ferromagnetic and paramagnetic contaminants at both fields to the expression susceptibility $\chi = A/T + B$, with the assumption that $\chi \approx 0$ for **1** below 30 K. The susceptibility vs temperature data for the compound, after subtracting the contaminants, are shown in Figure 2. We have analyzed these data using eq 1, dropping the hyperfine terms.

Although the determining parameter for $\chi(T)$ is the exchange coupling constant J , the zero-field splittings and the g values have some influence on χ . Given the similarity of the local sites of **1** with that of Rd_{red} , we have used the above-quoted D and E/D values to fit the data of **1**. For the g values we have used $g_x = g_y = 2.08$ and $g_z = 2.00$ as determined by high-frequency EPR of $[\text{PPh}_4]_2[\text{Fe}(\text{SPh})_4]$;^{18,19} this synthetic complex has essentially the same hyperfine and zero-field splitting parameters as Rd_{red} (see Table 1 of ref 17). We have also varied the \mathbf{D}_j and \mathbf{g}_j within reasonable bounds to assess to what extent the determination of J would be affected by these parameters.

As can be seen from an inspection of Figure 2, the 3.0 and 5.0 T data deviate slightly at temperatures above 150 K. This is not surprising given that the contribution of two unknown contaminants had to be subtracted from the raw data. However, the data obtained at both fields match well between 50 and 120 K, the temperature range where the susceptibility of $[\text{Fe}_2(\text{SEt})_6]^{2-}$ is most sensitive to J . From a series of simulations, we infer $J = 165 \pm 15 \text{ cm}^{-1}$. The quoted uncertainties were estimated by making various assumptions about the values of \mathbf{D}_j and \mathbf{g}_j and about the behavior of the impurities and by taking into account that the 3.0 and 5.0 T data differ slightly above 150 K for reasons not understood. The solid line in Figure 2 was obtained from eq 1 using the parameters listed in the caption of Figure 1.

(18) Knapp, M. J.; Krzystek, J.; Brunel, L.-C.; Hendrickson, D. N. *Inorg. Chem.* **2000**, *39*, 281.

(19) For a high-spin ferrous ion with an *isolated* orbital ground state, the \mathbf{g} - and \mathbf{D} -tensors are related,²⁰ which allows an estimation of the \mathbf{g} -tensor from the zero-field splittings. However, excited triplet states of the ferrous ion are admixed by spin-orbit coupling into the ground state, affecting the zero-field splitting. In contrast, the \mathbf{g} -tensor is not affected by the presence of triplet states. Analysis of the Rd_{red} data has shown that ca. 40% of the value of D is attributable to mixing with triplet states.¹⁷

Using $J = 165 \text{ cm}^{-1}$ we have simulated the 180 K Mössbauer spectrum of Figure 1C. Clearly, the larger J value of Figure 1C provides a better fit to the data than $J = 50 \text{ cm}^{-1}$ used to compute the curve of Figure 1D. Finally, the temperature independence of ΔE_Q shows that no excited orbital states are appreciably populated for $T < 300 \text{ K}$. Thus, the susceptibility of $[\text{Fe}_2(\text{SEt})_6]^{2-}$ reflects solely the spin ladder associated with the orbital ground state.

Discussion

The results reported here demonstrate that the planar Fe_2 - $(\mu\text{-SR})_2$ bridge unit with tetrahedral Fe(II) sites can sustain substantial antiferromagnetic coupling at an Fe-Fe separation of 3 Å. To date, the J value of **1** is the only measure of antiferromagnetic coupling by Fe^{2+} pairs in a tetrahedral sulfur environment. Although the J value determined here should provide a reasonable estimate for the exchange couplings of diferrous pairs in iron-sulfur clusters of higher nuclearity, some caution is advised. Thus, analysis of the spin-coupling of the all-ferrous Fe_4S_4 cluster of the Fe protein from *A. vinelandii* showed that the J values of different ferrous pairs differ by as much as a factor 3;⁷ however, the analysis provided only ratios of exchange couplings pertaining to different ferrous pairs, and thus the magnitude of the J values has still to be established. Using the broken symmetry method, Noodleman²¹ has estimated with density functional theory the J values of diferrous pairs in cubane clusters; his calculations suggest J values smaller than 100 cm^{-1} for $[\text{Fe}_4\text{S}_4]^+$, with indications of ferromagnetic coupling ($J < 0$) for the diferrous pair of $[\text{ZnFe}_3\text{S}_4]^+$. The multiparameter problem of $[\text{Fe}_4\text{S}_4]^{0,+}$ clusters renders determination of the J values of individual ferrous pairs exceedingly difficult. Perhaps, magnetic susceptibility studies of the *A. aeolicus* $[\text{Fe}_2\text{S}_2]$ ferredoxin reduced with Ti^{3+} citrate could provide a good opportunity for determining J for a sulfido-bridged diferrous pair.

In the literature, the exchange couplings of diferrous pairs are frequently assumed to be smaller than those of mixed-valence $\text{Fe}^{2+}\text{Fe}^{3+}$ pairs. It is therefore noteworthy that the J value of diferrous **1** is comparable to those reported for the mixed-valence state of the $[\text{Fe}_2\text{S}_2]^+$ clusters of plant-type ferredoxins ($150\text{--}200 \text{ cm}^{-1}$; see Table 3 of ref 22).

Ginsberg et al.²³ reported J values of ca. 50 and 100 cm^{-1} for two binuclear five-coordinate thiolate-bridged Fe(II) complexes with FeN_2S_3 coordination and Fe-Fe distances of 3.21 and 3.37 Å.²⁴ Their magnetic analysis involved the evaluation of orbitally dependent exchange pathways, with the consequence that their results are not directly comparable with the J value determined here. (As stated above, only the orbital ground state of **1** is measurably populated in our experiments.)

(20) Zimmermann, R.; Spiering, H.; Ritter, G. *Chem. Phys.* **1974**, *4*, 133.

(21) Noodleman, L. *Inorg. Chem.* **1991**, *30*, 246.

(22) Lloyd, S. G.; Franco, R.; Moura, J. J. G.; Moura, I.; Ferreira, G. C.; Huynh, B. H. *J. Am. Chem. Soc.* **1996**, *118*, 9892.

(23) Ginsberg, A. P.; Lines, M. E.; Karlin, K. D.; Lippard, S. J.; DiSalvo, F. J. *J. Am. Chem. Soc.* **1976**, *98*, 6958.

(24) Hu, W.; Lippard, S. J. *J. Am. Chem. Soc.* **1974**, *96*, 2366-2372.

Recently Hübner and Sauer²⁵ reported a theoretical study of the naked iron–sulfur clusters Fe₂S₂ in the gas phase, using complete active space self-consistent-field (CASSCF) with subsequent multireference configuration interactions (MRCI) calculations. The sulfide bridges provide a shorter Fe–Fe distance (2.59–2.64 Å calculated) than observed for

complex **1**, but the calculated $J = 140 \text{ cm}^{-1}$ is similar to that observed here.

Acknowledgment. This research was supported at Carnegie Mellon University by NSF Grant MCB-9904421 and at Harvard University by NIH Grant GM 28856.

(25) Hübner, O.; Sauer, J. *J. Chem. Phys.* **2002**, *116*, 617.

IC0204629